ISSN 1070-3284, Russian Journal of Coordination Chemistry, 2009, Vol. 35, No. 11, pp. 844–849. © Pleiades Publishing, Ltd., 2009.

Synthesis, Structure, and Electrochemical Behavior of a Novel Copper Compound $[Cu(2,2'\text{-Bipy})_3]_3(P_2W_{18}O_{62}) \cdot 2H_2O$[1]

J. Wang[a], X. Tang[a], F. Wang[b], and S. Cheng[a,*]

[a] *College of Chemistry and Chemical Engineering, Hubei University, Wuhan 430062, P.R. China*

[b] *School of Materials Science and Engineering, Jiangsu University of Science and Technology, Zhenjiang 212003, P.R. China*

**E-mail: scheng@public.wh.hb.cn*

Received January 17, 2009

Abstract—A novel copper compound constructed from Wells–Dawson polyanion clusters and metal-organic complex subunits,$[Cu(2,2'\text{-Bipy})_3]_3(P_2W_{18}O_{62}) \cdot 2H_2O$(I), has been prepared under hydrothermal conditions, and characterized by elemental analysis, IR, UV, TG, cyclic voltammetry, and single-crystal X-ray diffraction. Crystal structural analysis indicates that I crystallizes in triclinic system, space group $P\bar{1}$, $a = 15.6195(11)$, $b = 17.144(2)$, $c = 25.0900(15)$ Å, $\alpha = 93.1040(10)°$, $\beta = 94.309(3)°$, $\gamma = 102.642(2)°$. Three Cu^{2+} ions have the same coordination environment: Cu(1), Cu(2), and Cu(3) are all six-coordinated by three 2, 2'-Bipy. The Dawson polyoxoanion $[P_2M_{18}O_{62}]^{6-}$ do not coordinate with the Cu^{2+} ion added for charge balance.

DOI: 10.1134/S1070328409110098

INTRODUCTION

Polyoxometalates (**POM**) simultaneously exhibit many properties [1, 2] that make them attractive for applications in catalytic activity for chemical transformation [3], molecular conductivity [4], magnetism [5], luminescence, photochromism and electrochromism [6], etc. In these special properties, the great value for catalysis has attracted considerable interest, such as strong acidity, the ability to catalyze reversible redox reactions under mild conditions, fairly high stability in the solid state, etc. [7–9]. Tungsten-based Dawson-type compounds have recently been considered as suitable catalytic materials [10]. The design and synthesis of polyoxometalate-based hybrids are still at the forefront of the materials chemistry research, and the use of the well defined metal oxide clusters for the construction of polyoxometalate-based hybrid materials with more or less predictable connectivity in the crystalline state is more and more attractive. The hydrothermal synthesis techniques in combination with the organic templates have been demonstrated to be a popular strategy in the isolation of such materials [11–15]. Here, we report the hydrothermal synthesis, crystal structure, and characterization of this new Dawson polyoxotungstate $[Cu(2,2'\text{-Bipy})_3]_3(P_2W_{18}O_{62}) \cdot 2H_2O$ (**I**). Furthermore, the electrochemical behavior of the title compound is reported.

[1] The article is published in the original.

EXPERIMENTAL

Materials and physical measurement. All materials and organic solvents were of analytical grade and used without further purification. Distilled deionized water was used throughout. Elemental analyses (C, H, and N) were performed on a Perkin Elmer 2400 elemental analyzer. The infrared spectrum was recorded as a KBr pellet on a Nicolet 170SXFT-IR spectrometer in the 4000–500 cm^{-1} range. The electronic absorption spectra were taken on a Shimadzu UV-240 spectrophotometer. TG measurement was carried out on a Perkin Elmer 7 thermal analysis system in air with a heating rate of 10°C/min. Cyclic voltammograms were obtained on a model CHI660 electrochemical analyzer (CH Instruments, Austin, TX, USA) controlled by a personal computer at room temperature. A three-electrode system was used for the measurements, with a bare GCE (3 mm diameter) or C-Ni/GCE used as the working electrode, a saturated calomel electrode as the reference electrode, and a platinum wire as the auxiliary electrode. All experiments were performed at room temperature.

Synthesis of compound I. A mixture of $Na_2WO_4 \cdot 2H_2O$ (0.9857 g, 2.99 mmol), H_3PO_4 (0.3 ml, 85%), $Cu(CH_3COO)_2 \cdot H_2O$ (0.0385 g, 0.19 mmol), 2,2'-Bipy (0.0781 g, 0.50 mmol), and H_2O (15 ml) was stirred for half an hour in air, and pH value of the solution was adjusted to 4.1 by the addition of KOH (0.5 M) solution. The mixture was then transferred to a Teflon-lined stainless steel autoclave (25 ml) and kept at 170°C for 5 days. After the autoclave had cooled to room temperature, green block-shaped crystals were filtered off, washed

with distilled water, and air-dried to give a yield of 15% based on W.

For $C_{90}H_{76}Cu_3N_{18}O_{64}P_2W_{18}$			
anal. calcd, %:	C, 18.02;	H, 1.27;	N, 4.20.
Found, %:	C, 18.04;	H, 1.34;	N, 4.21.

X-ray structure determination. Single-crystal X-ray crystallographic analysis of **I** with approximate dimensions $0.14 \times 0.16 \times 0.20$ mm^3 was performed at 291(2) K on a Bruker SMART APEX CCD sealed tube diffractometer with graphite monochromated MoK_α radiation ($\lambda = 0.71073$ Å). Data collection, indexing, and initial cell refinements were carried out using the SMART software [16]. Frame integration and final cell refinements were carried out using the SAINT software [17]. Absorption corrections for each data set were applied using SADABS [18]. Structure solution, refinement, and generation of publication materials were performed using SHELXTL-97 [19]. Anisotropic thermal parameters were used to refine all non-hydrogen atoms except several oxygen, carbon, and nitrogen atoms. Hydrogen atoms were located at their ideal positions as a riding model. The crystallographic data and structure determination parameters for I are summarized in Table 1. Selected bond distances are given in Table 2. More details on the crystallographic studies, as well as atom displacement parameters, are presented in the Supporting Information.

RESULTS AND DISCUSSION

Hydrothermal reactions have been utilized successfully to synthesize great deal of novel organic–inorganic hybrid materials, although the syntheses and complete characterization of the polyoxometallates are not easy. In principle, the hydrothermal technique has many variables, which can affect the result significantly, such as the kind and stoichiometry of starting materials, temperature, pH, filling volume and reaction time, which can affect the result. Many research groups used Wells–Dawson POM α-$K_6P_2W_{18}O_{62} \cdot nH_2O$ as the precursor to prepare organic-inorganic hybrid complexes. In our experiments, we used $Na_2WO_4 \cdot 2H_2O$ and H_3PO_4 as starting materials instead of α-$K_6P_2W_{18}O_{62} \cdot nH_2O$, obtained a great product, suggesting that $Na_2WO_4 \cdot 2H_2O$ and H_3PO_4 as starting materials to synthesize hybrid compounds is also an effective strategy.

Single crystal X-ray diffraction analysis reveals that compound **I** is composed of three discrete $[Cu(2,2'\text{-Bipy})_3]^{2+}$ cations, two free water molecules, and the Dawson polyoxoanion $[P_2M_{18}O_{62}]^{6-}$ added for charge balance (Fig. 1). $[P_2W_{18}O_{62}]^{6-}$ in I has normal Wells–Dawson structure and are built up from edge- and corner-sharing octahedral encapsulating two phosphorus atoms (Fig. 2). Oxygen atoms in $[P_2W_{18}O_{62}]^{6-}$ can be divided into four groups according to their coordination

Table 1. Crystallographic data and details of the experiment and refinement of structures **I**

Parameter	Value
Crystal system	Triclinic
Space group	$P\bar{1}$
Unit cell dimensions:	
a, Å	15.6195(11)
b, Å	17.144(2)
c, Å	25.0900(15)
α, deg	93.1040(10)
β, deg	94.309(3)
γ, deg	102.642(2)
V, Å^3	6519.9(11)
Z	2
Absorption coefficient, mm^{-1}	16.401
F(000)	5406
Crystal size, mm	$0.20 \times 0.16 \times 0.14$
θ range for data collection, deg	2.11–23.72
Index ranges	$-19 \le h \le 19$, $-21 \le k \le 21$, $-19 \le l \le 30$
Reflections collected	61095
Unique reflections	25634
Reflections with $I > 2\sigma(I)$	18951
GOOF	1.030
Parameters	1792
Final R indices ($I > 2\sigma(I)$)*	$R_1 = 0.0468$, $wR_2 = 0.0873$
R indices (all data)	$R_1 = 0.0726$, $wR_2 = 0.0923$
Residual electronic density (max/min), e Å^{-3}	1.795/–2.056

* $R_1 = \Sigma||F_o| - |F_c||/|F_o|$; $wR_2 = \Sigma[w(F_o^2 - F_c^2)^2]/\Sigma[w(F_o^2)^2]^{1/2}$; $w^{-1} = [\sigma^2(F_o)^2 + (0.0447P)^2]$, $P = (F_o^2 + 2F_c^2)/3$.

Table 2. Selected bond lengths of compound **I**

Bond	*d*, Å	Bond	*d*, Å
P(1)–O(59)	1.562(8)	P(2)–O(55)	1.575(8)
P(1)–O(60)	1.518(8)	P(2)–O(56)	1.492(8)
P(1)–O(61)	1.480(8)	P(2)–O(57)	1.490(8)
P(1)–O(62)	1.503(8)	P(2)–O(58)	1.500(8)
W(1)–O(1)	1.697(7)	W(2)–O(2)	1.682(7)
W(1)–O(58)	2.337(7)	W(2)–O(58)	2.390(7)
W(1)–O(19)	1.991(7)	W(2)–O(19)	1.860(7)
W(3)–O(3)	1.722(8)	W(4)–O(4)	1.679(7)
W(3)–O(58)	2.434(8)	W(4)–O(55)	2.330(7)
W(3)–O(20)	1.911(8)	W(4)–O(43)	1.871(8)
W(5)–O(5)	1.711(8)	W(6)–O(6)	1.753(8)
W(5)–O(55)	2.389(8)	W(6)–O(56)	2.417(7)
W(5)–O(44)	1.912(8)	W(6)–O(45)	1.830(8)
W(7)–O(7)	1.695(8)	W(8)–O(8)	1.677(8)
W(7)–O(56)	2.358(7)	W(8)–O(57)	2.428(8)
W(7)–O(46)	1.995(8)	W(8)–O(47)	1.870(7)
W(9)–O(9)	1.699(7)	W(10)–O(10)	1.707(7)
W(9)–O(57)	2.378(7)	W(10)–O(59)	1.884(7)
W(9)–O(48)	1.990(8)	W(10)–O(49)	2.346(8)
W(11)–O(11)	1.758(8)	W(12)–O(12)	1.707(7)
W(11)–O(59)	2.377(8)	W(12)–O(60)	2.432(8)
W(11)–O(50)	1.908(8)	W(12)–O(51)	1.879(7)
W(13)–O(13)	1.659(7)	W(14)–O(14)	1.702(8)
W(13)–O(60)	2.371(8)	W(14)–O(61)	2.412(8)
W(13)–O(52)	1.921(7)	W(14)–O(32)	1.770(7)
W(15)–O(15)	1.736(8)	W(16)–O(16)	1.692(8)
W(15)–O(61)	2.392(7)	W(16)–O(62)	2.324(7)
W(15)–O(54)	1.888(8)	W(16)–O(54)	1.969(8)
W(17)–O(17)	1.764(9)	W(18)–O(18)	1.603(8)
W(17)–O(62)	2.418(8)	W(18)–O(62)	2.405(7)
W(17)–O(51)	1.949(7)	W(18)–O(53)	1.922(8)
Cu(1)–N(1)	2.071(10)	Cu(2)–N(7)	2.142(10)
Cu(1)–N(2)	2.115(10)	Cu(2)–N(8)	1.994(10)
Cu(1)–N(3)	2.179(10)	Cu(2)–N(9)	2.018(11)
Cu(1)–N(4)	2.036(9)	Cu(2)–N(10)	2.026(10)
Cu(1)–N(5)	2.081(10)	Cu(2)–N(11)	2.082(10)
Cu(1)–N(6)	2.177(11)	Cu(2)–N(12)	2.007(12)
Cu(3)–N(13)	2.050(10)	Cu(3)–N(16)	1.974(10)
Cu(3)–N(14)	2.114(11)	Cu(3)–N(17)	2.067(11)
Cu(3)–N(15)	2.122(10)	Cu(3)–N(18)	2.102(10)

number [20]: O_t (terminal oxygen atoms connecting only one W atom), O_b (oxygen atoms located in the share corners between two W_3O_{13} units), O_c (oxygen atoms connecting edge sharing WO_6 octahedrons in the same W_3O_{13} unit), and O_a (oxygen atoms connecting the P heteroatom and three W atoms). Relevant W–O bond distances in the anion can be classified into three groups: W–O_t 1.603(8)–1.764(9), 1.817–2.022; W–O_a 2.324(7)–2.434(8) Å; W–O_a 2.324(7)–2.434(8) Å. Their mean bond distances are 1.702(4), 1.974(5), and 2.385(4) Å, respectively. These bond distances have a rule of W–O_t < W–$O_{b,c}$ < W–O_a, and they are in accord with those in the well-known α-Dawson type anions [21–27]. O_{cis}–W–O_{cis} bond angles vary from 65.9(3)–125.9(4)°, O_{trans}–W–O_{trans} bond angles vary from 142.8(4)°–174.2(3)°. For the PO_4 tetrahedron, the P–O distances are 1.480(8)–1.575(8) Å with an average bond distance of 1.515(8) Å, while OPO angles vary from 102.1(4)°–114.1(5)°. All these bond lengths and angles are within the normal ranges and in close agreement with those described in the literature [28–31]. The +6 oxidation state is also confirmed by the bond valence sum calculations [32], which give an average value of 6.155 for the calculated oxidation states of W. The result is consistent with the formula of the title compound given by X-ray structure determination.

Each Cu^{2+} site in discrete $[Cu(2,2'\text{-Bipy})_3]^{2+}$ cations is defined by six nitrogen atoms from three 2,2'-bipyridine molecules and formed a distorted CuN_6 octahedron (Fig. 3) with Cu(1)–N bond lengths of 2.036(9)–2.179(10) Å, the Cu(2)–N bond lengths are 1.994(10)–2.142(10) Å, and the Cu(3)–N bond lengths are 1.974(10)–2.122(10) Å, corresponding to their mean Cu–N length 2.110(1), 2.044(9), and 2.071(6) Å. The opposed N_{cis}–Cu–N_{cis} angles are 75.4(4)°–111.1(4)°, the N_{trans}–Cu–N_{trans} angles are 156.1(4)°–174.2(4)°. Furthermore, the dihedral angles among the three ideal 2,2'-bipyridine planes in $[Cu(1)(2,2'\text{-Bipy})_3]^{2+}$ are 84.11°, 87.75°, and 55.34°. For $[Cu(2)(2,2'\text{-Bipy})_3]^{2+}$, the three dihedral angles among the three ideal 2,2'-bipyridine planes are 86.18°, 69.02°, and 84.13° and for $[Cu(3)(2,2'\text{-Bipy})_3]^{2+}$ are 83.58°, 87.75°, and 88.99°. The results indicate that the three ideal planes in each $[Cu(2,2'\text{-Bipy})_3]^{2+}$ ion are not vertical to each other.

It is worth to note that all CuN_6 octahedra in the title compound have been distorted to some extent. The CuL_6 octahedra have the well-known electronic system, $(t_{2g})^6(d_{x^2-y^2})^1(d_{z^2})^2$, with D_{4h} configuration [33], the Jahn–Teller distortion of CuN_6 octahedra are different (Fig. 4). The Jahn–Teller distortion of $Cu(1)N_6$ and $Cu(2)N_6$ is strong: the axial distances (av. 2.17 and 2.11 Å) are significantly larger than the equatorial ones (av. 2.07 and 1.99 Å) (the differences are 0.10 and 0.12 Å). Meanwhile, the $Cu(3)N_6$ octahedra shows the weaker presence of the Jahn–Teller effect with the axial distances (av. 2.08 Å) and the equatorial ones (av. 2.02 Å). The axial distance is slight longer than the equatorial one (the difference is 0.06 Å). In a sum, con-

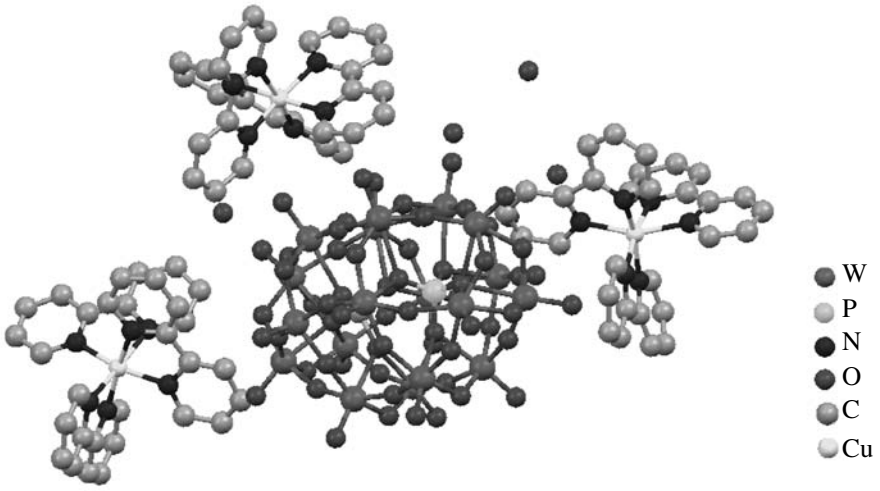

Fig. 1. Molecular structure of compound **I**. All hydrogen atoms are omitted for clarity.

sidering the different extent of the Jahn–Teller effect, it is expectable that the CuN_6 octahedra exhibit diverse distorted extent [33].

The IR spectra of the title compound exhibit the four characteristic W–O_t, P–O, W–O_b, and W–O_c, asymmetric stretching vibration peaks for heteropolyanions with the Dawson structure, these peaks appear at 1090, 956, 910, and 791 cm^{-1}. Comparing the IR spectra of the title compound with that of α-$H_6P_2W_{18}O_{62} \cdot nH_2O$ [34], the vibration band of W–O_d and W–O_b bonds have a red-shift of 5 and 2 cm^{-1}, respectively. The band of W–O_c has a bigger blue shift by 11 cm^{-1}, while the P–O bond appear nearly identical to that of α-$H_6P_2W_{18}O_{62} \cdot nH_2O$.

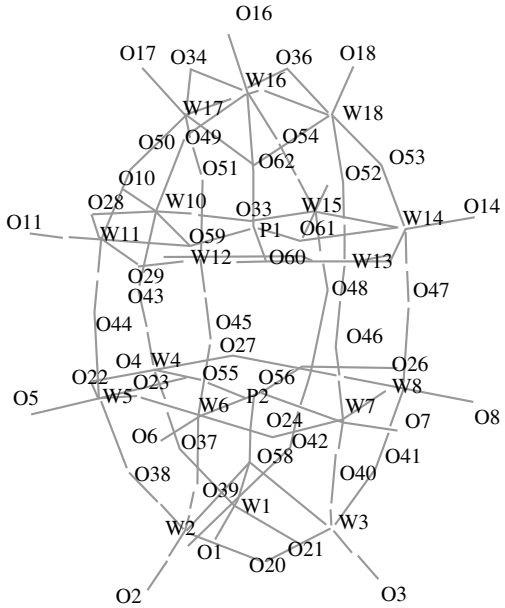

Fig. 2. Dawson polyoxoanion $[P_2W_{18}O_{62}]^{6-}$ in compound **I**.

These results indicate that the polyanions of the title compound still retains the basic Wells–Dawson structure but are distorted. The complex also shows characteristic bands of the 2,2'-Bipy ligand at 1440, 1471, and 1601 cm^{-1}. The peak at 3458 cm^{-1} can be assigned to the O–H stretching vibration of crystallization water or coordinated water molecules [35]. In addition, the weak peak at 3078 cm^{-1} may be attributed to the C–H stretching vibration of the heterocycle.

The UV spectra of the ligands and the title compound were obtained in a DMSO solution with DMSO as a reference (Fig. 5). An absorption band at 315 nm was observed, which may arise from the metal-to-ligand charge transfer [36]. The bands of 250 and 281 nm can be attributed to the $\pi \longrightarrow \pi^*$ transitions of the 2,2'-Bipy ligand. Furthermore, the maximum absorption band of Bipy at 280 nm is similar to that in the complex, but the molar extinction coefficient at the same wavelengths is greatly enhanced. Suggesting that

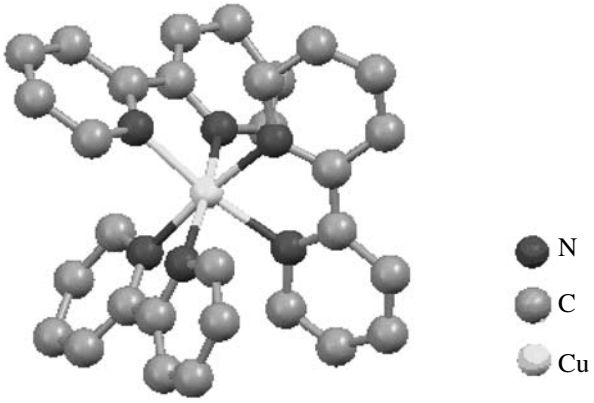

Fig. 3. Coordination environment of Cu in compound **I**.

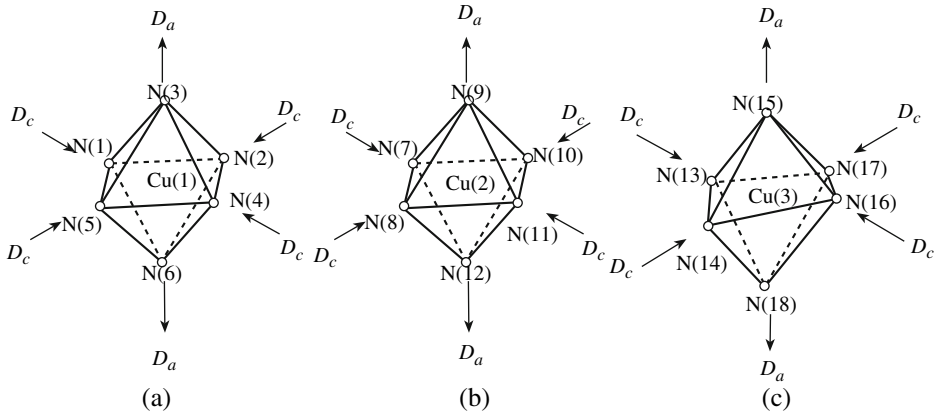

Fig. 4. View of the Jahn–Teller effect for different CuN_6 octahedra, D_a and D_e = mean axial equatorial distances, respectively: Cu(1) case, $D_a - D_e = 0.10$ Å (a); Cu(2) case, $D_a - D_e = 0.12$ Å (b); Cu(3) case, $D_a - D_e = 0.06$ Å (c).

it has even bigger conjugated system than the ligand, namely, forms the chelating ring [37].

A cyclic voltammogram obtained at a scan rate (v) of 100 mV s^{-1} for the reduction of the title compound (0.5 mM) in DMF 0.1 M H_2SO_4 at a glassy carbon macrodisk electrode over the potential range between 0.8 and –0.9 V, exhibits four chemically reversible processes (Fig. 6). Four reversible redox waves E_{pc} (–0.713, –0.483, –0.308, 0.025 V), E_{pa} (–0.684, –0.452, –0.274, 0.095 V), and $E_{1/2} = [(E_{pc} + E_{pa})/2]$ ($E_{1/2}$ = half-wave potential, E_{pc} = reduction peak potential, E_{pa} = oxidation peak potential) values of –0.698, –0.468, –0.291, and 0.060 V. The peak potential separations (ΔE_p) of the four pairs of redox peaks are 29, 31, 34, and 70 mV. Thus, the reversibility of $[P_2W_{18}O_{62}]^{6-}$ was significantly improved. For a reversible system, $\Delta E_p = E_{pa} - E_{pc} = 57\sim63/n$ (mV), using this formula, the electron transfer number n of the four redox steps can be calculated to be 2, 2, 2, and 1, respectively. The first two waves are independent of pH. Generally, cations in solution have no effect on the first two waves, thus when $[P_2W_{18}O_{62}]^{6-}$ is in solution, addition of the first two reversible reductions is not followed by protonation, while the third and fourth reversible reductions are accompanied by protonations [38]. The four reversible redox waves are summarized as show in Eqs. 1–4.

$$[P_2W_{18}O_{62}]^{6-} + 2e^- = [P_2W_{18}O_{62}]^{8-}, \quad (1)$$

$$[P_2W_{18}O_{62}]^{8-} + 2e^- = [P_2W_{18}O_{62}]^{10-}, \quad (2)$$

$$[P_2W_{18}O_{62}]^{10-} + 2e^- + 2H^+ = [H_2P_2W_{18}O_{62}]^{10-}, \quad (3)$$

$$[H_2P_2W_{18}O_{62}]^{10-} + e^- + H^+ = [H_3P_2W_{18}O_{62}]^{10-}. \quad (4)$$

The TGA measure (Fig. 7) shows a two-step weight loss. The first loss of 2.03% occurs between room temperature and 350°C, corresponding to the loss of free water molecules (calc. 1.80%). The second weight loss of 23.37% occurs in the range of 350–900°C, resulting from the release of 2,2'-Bipy ligands (calc. 23.42%). The two slight and one strong exothermal peaks appear at 350 and 628°C, which shows the combustion of

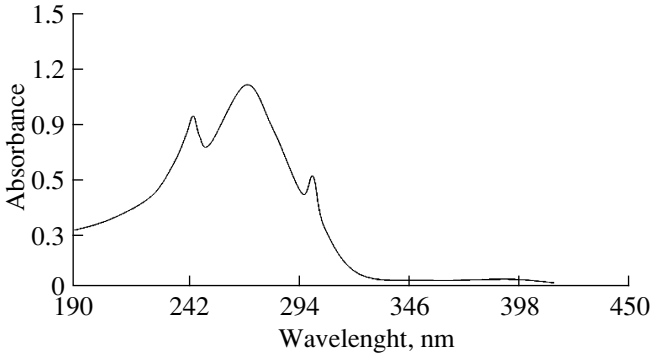

Fig. 5. UV spectra of compound **I** in DMSO.

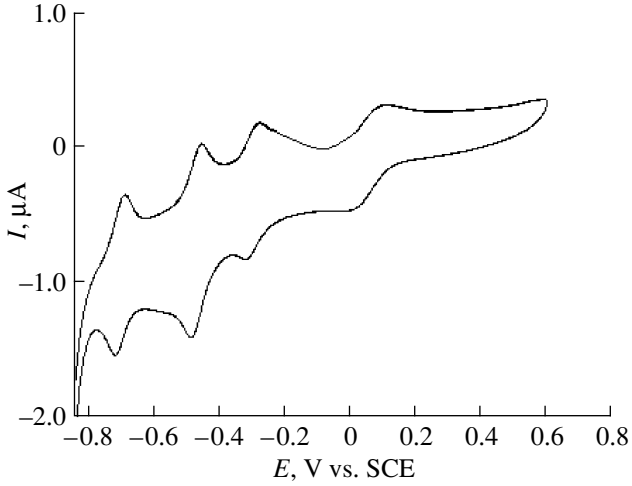

Fig. 6. Cyclic voltammograms of **I** (0.5 mM) in DMF + 0.1 M H_2SO_4; scan rate is 100 mV s^{-1}; working electrode is glassy carbon disk.

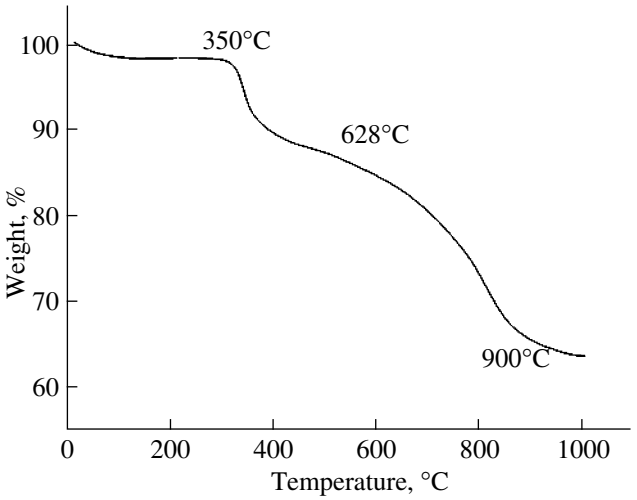

Fig. 7. TG curves of the title compound.

organic ligands and the decomposition of the polyanion framework.

Crystallographic data for the structure reported in this paper have been deposited with the Cambridge Crystallographic Data Centre as supplementary publication (no.706810; deposit@ccdc.cam.ac.uk or http://www.ccdc.cam.ac.uk).

REFERENCES

1. *Polyoxometalates*, Pope, M.T. and Muller, A., Eds., Dordrecht: Kluwer academic publications, 1994.
2. Hill, C.L., *Chem. Rev.*, 1998, vol. 98, p. 1.
3. Branytska, O.V. and Neumann, R.J., *Org. Chem.*, 2003, vol. 68, p. 9510.
4. Coronado, E., Galan-Mascaros, J.R., and Gimenez-Saiz, C., *Adv. Mater.*, 2004, vol. 16, p. 324.
5. Coronado, E., Clemente-Leon, M., and Galán-Mascaros, J.R., *Dalton, Trans.*, 2000, vol. 21, p. 3955.
6. Yamase, T., *Mol. Eng.*, 1993, vol. 3, p. 241.
7. Kozhevnikov, I., *Catal. Rev. Sci. Eng.*, 1995, vol. 37, p. 311.
8. Kozhevnikov, I., *Chem. Rev.*, 1998, vol. 98, p. 171.
9. Cavani, F., *Catal. Today*, 1998, vol. 41, p. 73.
10. Arendt, E., McEvoy, K.M., and Gaigneaux, E.M., *Appl. Catal., A*, 2009, vol. 357, no. 2, p. 115.
11. Hagrman, P.J., Hagrman, D., and Zubieta, J., *Angew. Chem. Int. Ed.*, 1999, vol. 38, p. 2638.
12. Reinoso, S., Vitoria, P., San, L.F., et al., *Chem. Eur. J.*, 2005, vol. 11, p. 1538.
13. Wang, C.-M., Zeng, Q.-X., Zhang J., and Yang G.-Y., *J. Cluster Sci.*, 2005, vol. 16, p. 65.
14. Zheng, P.-Q., Ren, Y.-P., Long, L.-S., et al., *Inorg. Chem.*, 2005, vol. 44, p. 1190.
15. Han, Z.-G., Zhao, Y.-L., Peng, J., et al., *Eur. J. Inorg. Chem.*, 2005, vol. 15, p. 264.
16. S*MART, Version 5.624*, Madison (WI, USA): Brüker AXS, Inc., 2002.
17. *SAINT, Version 6.36 A*, Madison (WI, USA): Brüker AXS, Inc., 2002.
18. Sheldrick, G.M, *SADABS*, *Version 2.10*, Göttingen (Germany): Univ. of Göttingen, 2003.
19. Sheldrick, G.M., *SHELXTL-97, Program for Crystal Structure Refinement*, Göttingen (Germany): Univ. of Göttingen, 1997.
20. Niu, J.-Y., Wang, Z.-L., and Wang, J.P., *Inorg. Chem. Commun.*, 2003, vol. 6, p. 1272.
21. Yan, B., Xu, Y., Bu, X.-H., et al., Dalton Trans., 2001, vol. 10, p. 2009.
22. Wei, M.-L., Liu, Y.-H., Guo, D.-J., and Wang, J.-P., *Chem. Res.*, 2003, vol. 14, p. 22.
23. Wang, J.-P., Zhao, J.-W., and Niu, J.-Y., *Mol. Struct.*, 2004, vol. 697, p. 191.
24. Dawson, B., *Acta Crystallogr.*, 1953, vol. 6, p. 113.
25. Krebs, B., Droste, E., Piepenbrink, M., et al., *Sci. Paris, Serie IIc.*, 2000, vol. 3, p. 205.
26. Mbomekalle, I.M., Keita, B., Nadjo, L., et al., D*alton Trans.*, 2003, vol. 10, p. 2646.
27. Nomiya, K., Torii, H., Nomura, K., and Sato, Y., *Dalton Trans.*, 2001, vol. 10, p. 1506.
28. Niu, J.-Y., Guo, D.-J., Wang, J.-P., and Zhao, J.W., *Cryst. Growth Des.*, 2004, vol. 4, p. 241.
29. Niu, J.-Y., Guo, D.-J., Zhao, J.-W., and Wang, J.-P., *New J. Chem.*, 2004, vol. 28, p. 980.
30. Wang, J.-P., Zhao, J.-W., and Niu, J.-Y., *Mol. Struct.*, 2004, vol. 697, p. 191.
31. Soumahoro, T., Burkholder, E., Ouellette, W., and Zubieta, J., *Inorg. Chim. Acta*, 2005, vol. 358, p. 606.
32. Brown, I.D. and Altermatt, D., Acta Crystallogy, *B*, 1985, vol. 41, p. 244.
33. Wang, J. -P., Wang, W., and Niu, J.-Y., *Inorg. Chem. Commun.*, 2007, vol. 10, p. 520.
34. Zhou, Y.-S., Peng, J., and Wang, E.-B., *Transition Met. Chem.*, 1998, vol. 23, p. 125.
35. Lis, S., *J. Alloys Compd.*, 2000, vol. 88, p. 300.
36. Zhang, K.-L., *Mol. Struct.*, 2005, vol. 779, p. 11.
37. Zhang, H.-Y., *J. Alloys Compd.*, 2008, vol. 464, p. 277.
38. Sadakane, M. and Steckhan, E., *Chem. Rev.*, 1998, vol. 98, p. 219.